

Young's double slit interference with vortex source

Qilin Duan(段琦琳), Pengfei Zhao(赵鹏飞), Yuhang Yin(殷玉杭), and Huanyang Chen(陈焕阳)
Citation: Chin. Phys. B, 2024, 33 (**1**): 014202. DOI: 10.1088/1674-1056/acfdfd
Journal homepage: http://cpb.iphy.ac.cn; http://iopscience.iop.org/cpb

What follows is a list of articles you may be interested in

Effective transmittance of Fabry-Perot cavity under non-parallel beam incidence

Yin-Sheng Lv(吕寅生), Pin-Hua Xie(谢品华), Jin Xu(徐晋), You-Tao Li(李友涛), and Hua-Rong Zhang(张华荣)
Chin. Phys. B, 2024, 33 (**1**): 014210. DOI: 10.1088/1674-1056/ad0ec3

Active control of surface plasmon polaritons with phase change materials

Yuan-Zhen Qi(漆元臻), Qiao Jiang(蒋瞧), Hong Xiang(向红), and De-Zhuan Han(韩德专)
Chin. Phys. B, 2023, 32 (**10**): 104202. DOI: 10.1088/1674-1056/accd5a

Bound states in the continuum in metal—dielectric photonic crystal with a birefringent defect

Hongzhen Tang(唐宏珍), Peng Hu(胡鹏), Da-Jian Cui(崔大健), Hong Xiang(向红), and Dezhuan Han(韩德专)
Chin. Phys. B, 2022, 31 (**10**): 104209. DOI: 10.1088/1674-1056/ac6db6

High-sensitivity methane monitoring based on quasi-fundamental mode matched continuous-wave cavity ring-down spectroscopy

Zhe Li(李哲), Shuang Yang(杨爽), Zhirong Zhang(张志荣), Hua Xia(夏滑), Tao Pang(庞涛),Bian Wu(吴边), Pengshuai Sun(孙鹏帅), Huadong Wang(王华东), and Runqing Yu(余润磬)
Chin. Phys. B, 2022, 31 (**9**): 094207. DOI: 10.1088/1674-1056/ac5d33

Design of three-dimensional imaging lidar optical system for large field of view scanning

Qing-Yan Li(李青岩), Yu Zhang(张雨), Shi-Yu Yan(闫诗雨),Bin Zhang(张斌), and Chun-Hui Wang(王春晖)
Chin. Phys. B, 2022, 31 (**7**): 074201. DOI: 10.1088/1674-1056/ac4a67

Young's double slit interference with vortex source

Qilin Duan(段琦琳)[1,3,†], Pengfei Zhao(赵鹏飞)[1,†], Yuhang Yin(殷玉杭)[1], and Huanyang Chen(陈焕阳)[1,2,‡]

[1] *Institute of Electromagnetics and Acoustics and Department of Physics, College of Physical Science and Technology, Xiamen University, Xiamen* 361005, *China*

[2] *Jiujiang Research Institute of Xiamen University, Jiujiang* 332000, *China*

[3] *Department of Electrical and Computer Engineering, National University of Singapore*, 117583, *Singapore*

(Received 16 July 2023; revised manuscript received 21 August 2023; accepted manuscript online 28 September 2023)

The fast and convenient demultiplex of optical vortex (OV) mode is crucial for its further application. We propose a novel approach that combines classic Young's doublet with an OV source to effectively identify the OV mode through the analysis of interference patterns. The interference patterns of the OV source incident on the double slits can be perfectly illustrated by using both the classical double-slit interference method and the Huygens–Fresnel principle. The interference fringes will twist along the negative or positive direction of x axis when topological charge (TC) $l > 0$ or $l < 0$, and the degree of the movement varies with the TC, allowing for a quantitative display of the OV characteristics through the interference patterns. Additionally, we deduce analytically that the zeroth-order interference fringe has a linear relationship with the TC and the vertical position. These findings highlight the ability to identify the OV mode by analyzing the interference patterns produced by Young's doublet.

Keywords: Young's double slit, vortex source, inteference patterns

PACS: 42.25.Hz, 42.50.Tx **DOI:** 10.1088/1674-1056/acfdfd

1. Introduction

Young's double-slit experiment is one of the most classic and elegant experiments in physics.[1] This experiment serves as compelling evidence for the wave nature of light, electrons,[2] and molecules,[3] etc. The chiral versions of Young's double slit[4] and Young's double slit in time domain[5] have been proposed with the development of research. These adaptations have expanded our understanding of the phenomenon. Vortices widely exist in nature, such as the tropical cyclone and tornado. In the field of optics, optical vortices (OVs) with helical wavefronts can carry optical angular momentums (OAMs), which can be characterized by the phase expression $\exp(\mathrm{i}l\varphi)$, where φ is the azimuthal angle and l is the topological charge (TC).[6] Owing to the nonorthogonality and infinite number of eigenstates in the Hilbert space,[7] OVs exhibit vast potential for applications in communication[8,9] and information encoding.[10] The identification of the OV mode holds great importance in these applications. To address this, various interferometric devices[11–13] and diffractive devices with different apertures shapes[14,15] have been proposed. Notably, it is well known that Young's interference pattern in the far field emerges as a result of two contributing factors: the source coherence and the optical path difference between the observation point in screen and the double slit, thus the double-slit interference patterns can provide a quantitative means of visualizing and determining the OV source mode.

It has been reported that the double-slit interference patterns with traditional OAM-carrying waves exhibits distinctive twist to a certain direction that corresponds to the variation of the TC.[16,17] This phenomenon deviates from the conventional flat fringes. Besides the interaction of Laguerre–Gaussian beam with Young's double slit, the phenomenon of radially polarized vortex beams,[18] partially coherent vortex beam,[19] and a relativistic vortex laser[20] incident on the Young's double slit have been studied, and the interference patterns will exhibit a tilted nature. However, an OV source incident on the doublet still remains to be thoroughly investigated. The OV source can be regarded as possessing intrinsic OAM which is related to the spiral phase.[21,22] The generation of OVs has been reported, furthermore, OVs may avoid certain challenges commonly encountered by traditional OAM-carrying waves, such as the beam divergence with the increase of the transmission distance.[23,24] When an OV source incident on the doublet, it induces a phase difference at the two slits, which will lead to the twist of the interference fringes.

In this paper, we explain this phenomenon using both the classical double-slit interference method and the Huygens–Fresnel principle.[25] By considering these perspectives, we aim to shed light on the underlying mechanisms behind the observed twist in the interference patterns. For the classical double-slit interference method, the interference fringes can be derived by considering the optical path difference and the initial phase difference at the two slits. On the other hand,

†These authors contributed equally to this work.

‡Corresponding author. E-mail: kenyon@xmu.edu.cn

© 2024 Chinese Physical Society and IOP Publishing Ltd

in Huygens–Fresnel principle, the interference process can be interpreted as the superposition of two point sources located at the two slits with different phases. Remarkably, these two methods are consistent with each other. Moreover, by employing analytical deductions, we can establish a relationship between the position x corresponding to the maximum intensity and the TC. Particularly, through a rigorous equation derived from the classical double-slit interference method, we discover a linear correlation between the TC and position of the zeroth-order interference fringes. These phenomena are helpful for the demultiplex of the vortex mode via an extremely simple Young's doublet structure.

2. Theory

To begin with, the interference patterns on the screen when the OV source interacts with the double slit can be effectively demonstrated using the classical double-slit interference method. As shown in Fig. 1(a), the double slit located at S_1 and S_2 can be regarded as two new point sources when the OV source with TC $= l$ incident on the double slit. The OV source has the basic forms as follows:

$$H_{0Z}^{\text{inc}} = H_l^{(1)}(k_0 \cdot r)\exp(\mathrm{i}l\varphi), \tag{1}$$

where $H_l^{(1)}$ is the first kind Hankel function, k_0 is the vacuum wavevector, φ is the azimuthal angle, and l is the TC. The OV source with helical wavefront will introduce a phase difference in the double slits, thus the interference patterns on the screen are composed of both the optical path length and the influence of the OV source. The intensity of the interference fringes will be given by considering the two parts:[20]

$$I \propto \operatorname{sinc}^2\left(\frac{\pi x a}{\lambda D}\right)\cdot\cos^2\left(\frac{\delta}{2}+\frac{\Delta\varphi}{2}\right), \tag{2}$$

where a is the slit width chosen to be 0.018 m. The first term accounts for the diffraction of the two slits, each slit generates diffracted waves. The second term describes the interference process that arises when the diffracted waves from the two slits overlap and interact with each other. The optical path length difference δ between r_1 and r_2 is

$$\delta = k_0 n\frac{2xd}{\sqrt{D^2+(x-\frac{d}{2})^2}+\sqrt{D^2+(x+\frac{d}{2})^2}}, \tag{3}$$

and the OV source phase difference $\Delta\varphi$ between S_1 and S_2 is

$$\Delta\varphi = l\left[2\arctan\left(\frac{d}{2b}\right)\right]. \tag{4}$$

Here, n is the refractive index of the background ($n = 1$ for air), d is the length of the two slits, D is the distance between the screen and the double slits, and b is the length between the source and the double slits. The distance between the double slits and the screen is sufficiently large to allow for the observation of the far-field interference fringes on the screen. Moreover, the interference patterns can be analytically obtained by employing the Huygens–Fresnel principle. This approach considers two sources placed at the slits with different phases as represented in Eq. (4). By utilizing this theoretical framework, we can effectively capture and understand the formation of the interference patterns in a quantitative manner. Figures 1(b)–1(d) show the two methods to obtain the interference patterns for $l = -6$, 0, 6, respectively. The two methods employed to derive the intensity interference fringes are consistent with each other. As shown in Fig. 1(c), the interference patterns are symmetric with respect to the line $x = 0$ when $l = 0$, which is due to the identical phase distribution at the two slits. However, this symmetric distribution will be broken when $l = -6$, 6 as depicted in Figs. 1(b) and 1(d). This is attributed to the presence of the OV source, which introduces a distinct phase distribution at the doublet and breaks the inherent symmetry of the system. Consequently, the resulting interference patterns exhibit an asymmetrical distribution.

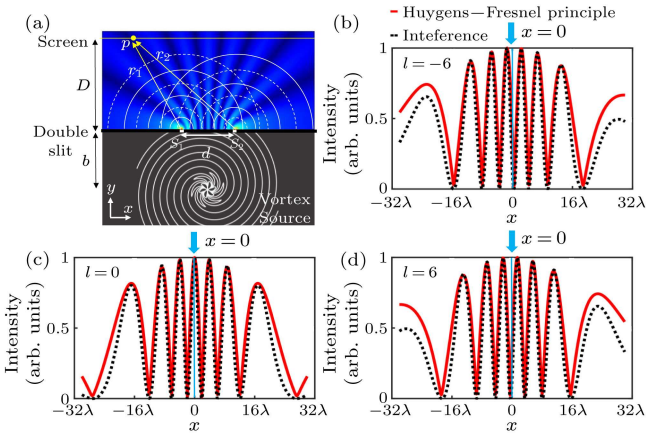


Fig. 1. The interaction of double slit with optical vortex (OV) source. (a) Schematic diagram of the double-slit interference with OV source, here $\lambda = 0.25$ m, $d = 4\lambda$, $b = 6\lambda$, and $D = 15\lambda$. (b)–(d) The normalized interference intensity at the screen with the OV source for $l = -6$, 0, 6 respectively. The red solid lines are acquired through the Huygens–Fresnel principle, and the black dotted lines correspond to the classical double-slit interference method.

The interference fringes derived from the classical double-slit interference method is a classical and intuitive way. To better study the variation of the interference patterns with different TCs, we show the full interference patterns analytically according to the Huygens–Fresnel principle in Figs. 2(a)–2(c) for $l = -6$, 0, 6 respectively. Here the parameters are the same as those in Fig. 1. As shown in Fig. 2(b), the interference pattern is symmetrical with x position for $l = 0$, while the interference patterns will twist to different directions for $l = -6$, 6 as shown in Figs. 2(a) and 2(c). To quantitively observe the deviation of the interference fringes, the normalized analytical and numerical intensity patterns at the screen are also shown in Figs. 2(d)–2(f). Here the blue

lines in Figs. 2(d)–2(f) are the numerical results acquired from the simulation. We perform the simulations through commercial software COMSOL MULTIPHYSICS and the transverse magnetic (TM) mode (E_x, E_y, H_z) is considered. Meanwhile, we use the Huygens–Fresnel principle to get the analytical results represented by the dotted red lines. Note that the polarization mode will not influence the far-field interference patterns and the slit thickness will only affect the intensity of the fringes rather than the positions of the interference fringes.[26] For simplicity, we consider the double slits composed of perfect electric conductor (PEC). Here the analytical and numerical interference fringes are consistent with each other, in which the x position of the maximum intensity is obviously unchanged.

The corresponding fast Fourier transforms (FFTs) shown in Figs. 2(g)–2(i) also exhibit the characteristics of the interference patterns for different TCs vividly. The isotropic and continuous FFT dispersions in air will become discrete due to the interference of the two sources at the double slits as shown in Fig. 2(g) for $l = 0$, while the FFT dispersions for $l = -6$ and $l = 6$ will separately twist to the right and left side as shown in Figs. 2(g) and 2(i). Thus, the interference fringes of the OV source passing through the double slit have the potential to distinguish different modes of vortex source. Moreover, the simplicity of the structure required to achieve this distinction is noteworthy. The double slit configuration is straightforward and can be easily fabricated, making it an attractive and accessible option for studying and analyzing OV.

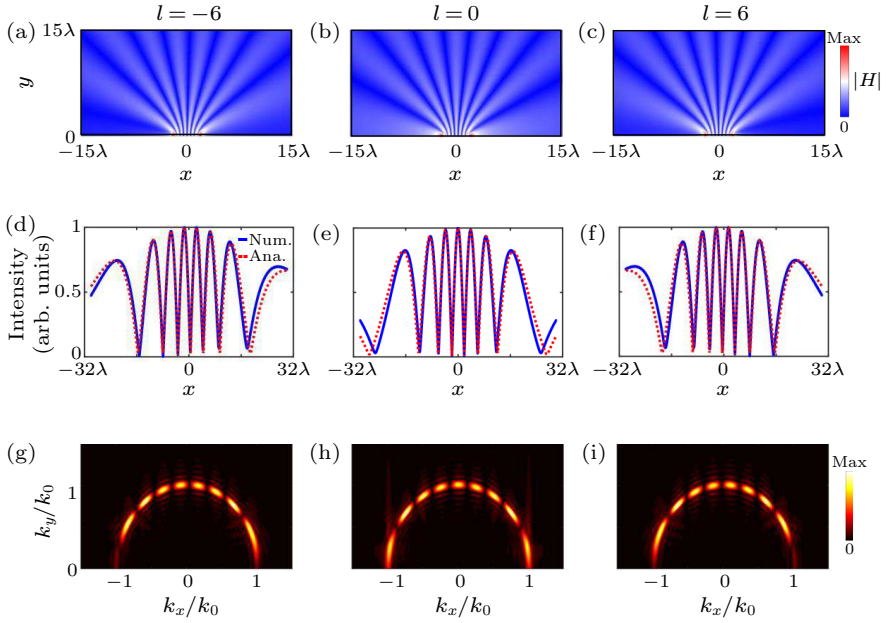


Fig. 2. Double-slit interference patterns with OV. (a)–(c) Analytical field patterns obtained through the Huygens–Fresnel principle for the OV source with $l = -6$, 0, 6 respectively. (d)–(f) the numerical/analytical normalized interference intensity at the screen for $l = -6$, 0, 6 respectively. (g)–(i) The FFT patterns for (a)–(c), respectively.

3. Results and discussion

To quantitively study the interference patterns with the variation of l and x, the absolute value of the field at the screen is extracted as shown in Fig. 3. For Young's double slit configurations, the length d between the slits S_1 and S_2 will have greater impact on the interference patterns among the geometrical parameters in Fig. 1(a). As shown in Figs. 3(a) and 3(b), the number of bright fringes will increase when d becomes larger, which is due to the spacing of interference fringes that becomes smaller. In Fig. 3, it can be observed that all the bright fringes will move towards the negative direction with the increase of TC, which shows the potential to identify the OV mode through interference patterns.

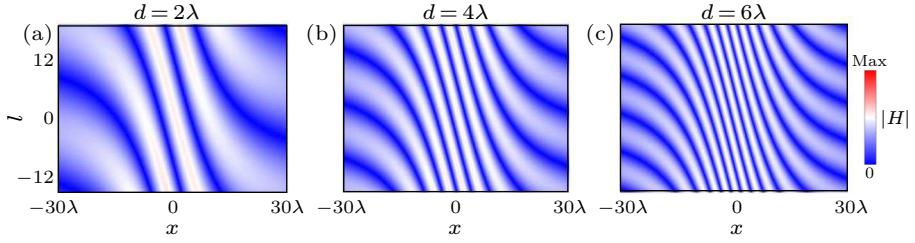


Fig. 3. Shifting of the analytical interference fringes obtained through the Huygens–Fresnel principle on the screen with the different lengths of the slit: (a) $d = 2\lambda$, (b) $d = 4\lambda$, and (c) $d = 6\lambda$.

To further characterize the OV mode, here we aim to derive the relationship between TC and x for the bright fringes. Surprisingly, this relationship can be derived by the aid of classical double-slit interference method. The bright fringes correspond to the constructive interference, which requires $\frac{\delta}{2}+\frac{\Delta\varphi}{2}=2A_1\pi$, thus the relationship between the TC and x can be written as

$$x=-\lambda(c_3 l-2\pi A_1)\times\frac{\sqrt{4\{c_1^2c_2-c_3^2d^2\lambda^2l^2+4d^2\lambda^2(c_3l\pi A_1-\pi^2A_1^2)\}+c_1^2d^2}}{\sqrt{-c_1^2\left(-c_1^2+4c_3^2\lambda^2l^2-16c_3\lambda^2l\pi A_1+16\lambda^2\pi^2A_1^2\right)}}. \tag{5}$$

Here $A_1=0.5N$ $(N\in Z^{\cdot})$, $c_1=2\pi d$, $c_2=D^2$, $c_3=\arctan(\frac{d}{2b})$. As shown in Fig. 4(a), the black and red circles represent the expression given by Eq. (5), which is consistent with the maximum intensity of the bright fringes. Particularly, the red circles correspond to the $A_1=0$, which can be regarded as the zeroth-order interference fringes. When $A_1=0$, Eq. (5) can be simplified, by leveraging the Taylor expansion $\arctan(\frac{d}{2b})\sim\frac{d}{2b}$ since b is larger than d, to

$$x=-\frac{d\lambda l\sqrt{-\frac{d^4\lambda^2l^2}{b^2}+4d^2\pi^2(d^2+4D^2)}}{4b\pi\sqrt{d^4\left(-\frac{\lambda^2l^2}{b^2}+4\pi^2\right)}}. \tag{6}$$

Note that the superoscillations radius of OV source is $r=l/k_0$ according to Berry's theory,[27] thus b should be set to be larger than the wavelength to effectively test the value of TC. Since D is also larger than d, and b should be set to be larger than the wavelength, a simple linear relationship can be derived as follows:

$$x=-l\frac{\lambda D}{2b\pi}. \tag{7}$$

Next, we aim to prove the accuracy of the simplified Eq. (7). In Figs. 4(b)–4(d), the relationship between x and other parameters are plotted using Eq. (5) (black dotted lines) and Eq. (7) (red dotted lines). Firstly, as shown in Fig. 4(b), clearly the two results are consistent with each other, which proves the accuracy of Eq. (7). The coefficient of linear relation in Eq. (7) is related to D and b when the wavelength and TC are fixed. It can be predicted from Eq. (7) that x has an inverse proportional relationship with b while varies proportionally with D. As shown in Fig. 4(c), the deviation x has an inverse proportional relationship with b when $l=-6$. The linear relationship between the x and D is shown in Fig. 4(d). Figures 4(c) and 4(d) both show the consistency between the simplified Eq. (7) and the original solutions manifested by Eq. (5). Above all, the zeroth-order bright interference fringes has a strict linear relationship with TC, which can be applied to distinguish different OV modes through simple Young's double slits.

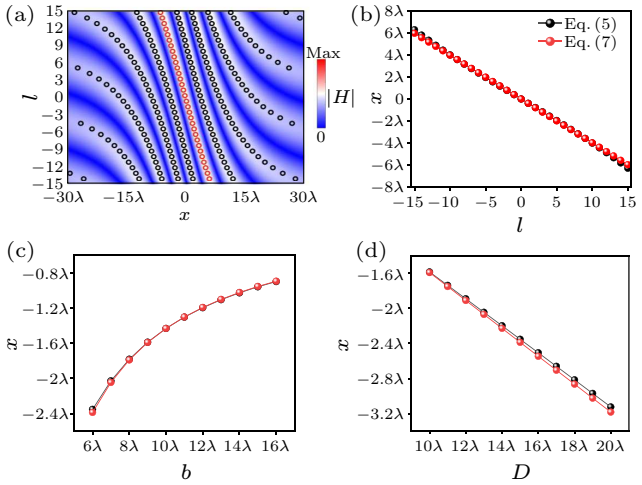


Fig. 4. The linear relationship of the zeroth-order interference field between the TC and the position x. (a) The field patterns for different x and l, the black and red circle is the analytical solution of Eq. (5). (b) The analytical results of the linear relationship with topological charge l and the position x manifested by Eqs. (5) and (7). (c) The analytical results of the inverse proportional relationship with b and the position x for $l=-6$. (d) The analytical results of the relationship with D and the position x for $l=-6$.

4. Conclusion and perspectives

In summary, we have investigated the interference patterns of OV source passing through the double slit. We employ the classical double-slit interference method that uses phase difference of optical paths to investigate the interference patterns. Additionally, we also utilize the analytical method based on the Huygens–Fresnel principle to obtain the interference patterns. This analytical method provides a complementary perspective to the classical double-slit interference method. To further verify the accuracy of the two methods, numerical simulation is also performed. Indeed, all three approaches yield consistent results for the interference patterns, providing a coherent and unified understanding of the interference phenomenon. The bright interference fringes will be antisymmetric since the different TC will introduce initial phase difference at the two slits. A simple linear relationship at the far-field screen between x and TC can be derived from the classical double-slit interference method, which can be used to quantitively measure the TC of the OV source. Meanwhile, the findings in this study will expand the understanding about the OV and Young's doublet. Above all, our results provide a simple configuration to measure the mode of the OV source, which will have potential applications in the future on-chip optical communications and optical detection. In addition, it may also be possible to extend the concept to acoustic waves[28] and surface water waves[29] in future.

Acknowledgements

Project supported by the National Key Research and Development Program of China (Grant Nos. 2020YFA0710100

and 2023YFA1407100), the National Natural Science Foundation of China (Grant Nos. 92050102 and 12374410), the Jiangxi Provincial Natural Science Foundation (Grant No. 20224ACB201005), the Fundamental Research Funds for the Central Universities (Grant Nos. 20720230102 and 20720220033), and China Scholarship Council (Grant No. 202206310009).

References

[1] Young T 1802 *Trans. R. Soc. Lond.* **92** 12
[2] Frabboni S, Gazzadi G C and Pozzi G 2007 *Am. J. Phys.* **75** 1053
[3] Schmidt L Ph H, Schössler S, Afaneh F, Schöffler M, Stiebing K E, Schmidt-Böcking H and Dörner R 2008 *Phys. Rev. Lett.* **101** 173202
[4] Ayuso D, Ordonez A F, Decleva P, Ivanov M and Smirnova O 2021 *Nat. Commun.* **12** 3951
[5] Tirole R, Vezzoli S, Galiffi E, Robertson I, Maurice D, Tilmann B, Maier S A, Pendry J B and Sapienza R 2023 *Nat. Phys.* **19** 999
[6] Allen L, Beijersbergen M W, Spreeuw R J C and Woerdman J P 1992 *Phys. Rev. A* **45** 8185
[7] Chen R, Zhou H, Moretti M, Wang X and Li J 2020 *IEEE Commun. Surv. Tutor.* **22** 840
[8] Liu B Y, Cui Y H and Li R L 2017 *IEEE Anten. Wireless Propag. Lett.* **16** 744
[9] Hui X, Zheng S, Chen Y, Hu Y, Jin X, Chi H and Zhang X 2015 *Sci. Rep.* **5** 10148
[10] Fang X, Ren H and Gu M 2020 *Nat. Photon.* **14** 102
[11] Ren Y, Qiu S, Liu T and Liu Z L 2022 *Nanophotonics* **11** 1127
[12] Gao C, Qi X, Liu Y, Xin J and Wang L 2011 *Opt. Commun.* **284** 48
[13] Huang H, Ren Y, Yan Y, Ahmed N, Yue Y, Bozovich A, Erkmen B I, Birnbaum K, Dolinar S, Tur M and Willner A E 2013 *Opt. Lett.* **38** 2348
[14] Chen X Y, Zhang A, Liu J M, Xie Z Q, Su M Y, He Y L, Zhou X X, Chen Y, Li Y, Chen S Q and Fan D Y 2019 *J. Opt.* **21** 065603
[15] Hickmann J M, Fonseca E J S, Soares W C and Chávez-Cerda S 2010 *Phys. Rev. Lett.* **105** 053904
[16] Sztul H I and Alfano R R 2006 *Opt. Lett.* **31** 999
[17] Emile O and Emile J 2014 *Appl. Phys. B* **117** 487
[18] Qi J, Wang W, Li X, Wang X, Sun W, Liao J and Nie Y 2014 *Opt. Eng.* **53** 044107
[19] Chen T, Lu X, Zeng J, Wang Z, Zhang H, Zhao C, Hoenders B J and Cai Y 2020 *Opt. Express* **28** 38106
[20] Zhang H, Shen B F and Zhang L G 2019 *Chin. Phys. B* **28** 014702
[21] Duan Q, Yin Y, Han L, Zhu S, Zhou Y, Chen H and Chen H 2023 *Adv. Opt. Mater.* **11** 2202111
[22] Chen J, Wan C and Zhan Q W 2021 *Adv. Photon.* **3** 064001
[23] Zheng S, Chen Y, Zhang Z, Jin X, Chi H, Zhang X and Chen Z N 2018 *IEEE Trans. Anten. Propag.* **66** 1352
[24] Zhang Z, Zheng S, Jin X, Chi H and Zhang X 2016 *IEEE Anten. Wireless Propag. Lett.* **16** 8
[25] Peatross J and Ware M 2010 *Physics of light and optics: A free online textbook.* In: *Frontiers in Optics 2010/Laser Science XXVI* (Optical Society of America) p. JWA64
[26] Teng S, Li F, Wang J and Zhang W 2013 *J. Opt. Soc. Am. A* **30** 2273
[27] Berry M V 2013 *J. Opt.* **15** 044006
[28] Fan X D, Zou Z and Zhang L 2019 *Phys. Rev. Res.* **1** 032014
[29] Han L, Chen S and Chen H 2022 *Phys. Rev. Lett.* **128** 204501